Cardiomyocytes capture stem cell-derived, anti-apoptotic microRNA-214 via clathrin-mediated endocytosis in acute myocardial infarction

Received for publication, January 14, 2019, and in revised form, June 17, 2019 Published, Papers in Press, June 19, 2019, DOI 10.1074/jbc.RA119.007537

Shunsuke Eguchi, Mikito Takefuji[1], Teruhiro Sakaguchi, Sohta Ishihama, Yu Mori, Takuma Tsuda, Tomonobu Takikawa, Tatsuya Yoshida, Koji Ohashi, Yuuki Shimizu, Ryo Hayashida, Kazuhisa Kondo, Yasuko K. Bando, Noriyuki Ouchi, and Toyoaki Murohara[2]

From the Department of Cardiology, Nagoya University School of Medicine, Nagoya, Japan, 65 Tsurumai, Showa, Nagoya 466-8550, Japan

Edited by Roger J. Colbran

Extracellular vesicles (EVs) have emerged as key mediators of intercellular communication that have the potential to improve cardiac function when used in cell-based therapy. However, the means by which cardiomyocytes respond to EVs remains unclear. Here, we sought to clarify the role of exosomes in improving cardiac function by investigating the effect of cardiomyocyte endocytosis of exosomes from mesenchymal stem cells on acute myocardial infarction (MI). Exposing cardiomyocytes to the culture supernatant of adipose-derived regenerative cells (ADRCs) prevented cardiomyocyte cell damage under hypoxia *in vitro*. *In vivo*, the injection of ADRCs into the heart simultaneous with coronary artery ligation decreased overall cardiac infarct area and prevented cardiac rupture after acute MI. Quantitative RT-PCR–based analysis of the expression of 35 known anti-apoptotic and secreted microRNAs (miRNAs) in ADRCs revealed that ADRCs express several of these miRNAs, among which miR-214 was the most abundant. Of note, miR-214 silencing in ADRCs significantly impaired the anti-apoptotic effects of the ADRC treatment on cardiomyocytes *in vitro* and *in vivo*. To examine cardiomyocyte endocytosis of exosomes, we cultured the cardiomyocytes with ADRC-derived exosomes labeled with the fluorescent dye PKH67 and found that hypoxic culture conditions increased the levels of the labeled exosomes in cardiomyocytes. Chlorpromazine, an inhibitor of clathrin-mediated endocytosis, significantly suppressed the ADRC-induced decrease of hypoxia-damaged cardiomyocytes and also decreased hypoxia-induced cardiomyocyte capture of both labeled EVs and extracellular miR-214 secreted from ADRCs. Our results indicate that clathrin-mediated endocytosis in cardiomyocytes plays a critical role in their uptake of circulating, exosome-associated miRNAs that inhibit apoptosis.

Substantial improvements in primary prevention efforts to reduce risk factors of cardiovascular disease, including smoking, low-density lipoprotein cholesterol, and blood pressure, have decreased the incidence of myocardial infarction (MI)[3] (1); however, cardiovascular disease, including ischemic heart disease, remains the leading cause of mortality worldwide. Cell-based therapy represents a potential frontier to transform the treatment and prognosis of heart failure and acute myocardial infarction through repair of damaged cardiac tissue (2). Numerous early-phase randomized clinical trials have investigated the clinical benefits of cell transplantation in patients with acute MI. Bone marrow cells represent the most commonly utilized cellular source, although the beneficial effects of their transplantation in patients with MI are controversial (3). Recently, mesenchymal stem cells and cardiac progenitor cells have served as alternate cellular sources of cell-based therapy (4). Cardiac progenitor cells are capable of cardiac regeneration (5); moreover, their paracrine effects improve tissue resistance to ischemic stress (6). Mesenchymal stem cells produce and secrete a broad range of cytokines, chemokines, and growth factors that are potentially involved in cytoprotection and angiogenesis (7). In cell-based therapy, both cell types secrete paracrine factors in extracellular vesicles (EVs), such as exosomes and microvesicles, to improve cardiac function (8). The concept of EVs as messengers in intracellular communication implies that EVs secreted from endothelial cells and cardiac fibroblasts may interact with cardiomyocytes to induce physiological changes (4). Although EVs derived from endothelial cells, cardiac fibroblasts, and transplanted cells have emerged as key mediators of intercellular communication to improve cardiac function (9), the mechanisms by which cardiomyocytes effect transmembrane signaling in response to EVs remain unclear. Here, we report that clathrin-mediated endocytosis in cardiomyocytes plays a critical role in transporting circulating microRNAs (miRNAs) into the cell.

This work was supported by a Grant-in-Aid for Scientific Research from the Ministry of Education, Culture, Sports, Science and Technology of Japan (to M. T.). The authors declare that they have no conflicts of interest with the contents of this article.

[1] To whom correspondence may be addressed. Tel.: 81-52-744-2147; Fax: 81-52-744-2210; E-mail: takefuji@med.nagoya-u.ac.jp.

[2] To whom correspondence may be addressed. Tel.: 81-52-744-2147; Fax: 81-52-744-2210; E-mail: murohara@med.nagoya-u.ac.jp.

[3] The abbreviations used are: MI, myocardial infarction; ADRC, adipose-derived regenerative cell; miRNA, microRNA; BM-MNC, bone marrow mononuclear cell; BNP, brain natriuretic peptide; ANP, atrial natriuretic peptide; EV, extracellular vesicle; TTC, triphenyltetrazolium chloride; TUNEL, terminal deoxynucleotidyltransferase dUTP nick-end labeling; qRT-PCR, quantitative reverse transcription PCR; AP2, adaptor protein-2; AAK1, adaptor association kinase 1; NRVM, neonatal rat ventricular myocytes; DMEM, Dulbecco's modified Eagle's medium.

Results

Adipose-derived regenerative cells (ADRCs) protect against ischemia-induced cardiac dysfunction

To investigate whether mesenchymal stem cells effect cardiac protection through secretion of paracrine factors, isolated mouse adult cardiomyocytes under hypoxia conditions were treated with the supernatant of bone marrow-mononuclear cell (BM-MNC) or ADRC cultures (Fig. 1*A*). After 6-h exposure to normoxia or hypoxia, hypoxia-damaged cardiomyocytes were ascertained by trypan blue vital staining. Hypoxia decreased cardiomyocyte cell viability, whereas this response was more effectively ameliorated by treatment with the supernatant from ADRC culture than that from BM-MNCs.

To determine whether treatment with ADRCs might attenuate the progression of myocardial ischemia-induced cardiac dysfunction in mice, we ligated the left coronary artery in mice. ADRCs or BM-MNCs were injected in the heart simultaneously with coronary artery ligation, and infarct changes were determined in triphenyltetrazolium chloride (TTC)-stained sections 2 days after the ligation (Fig. 1*B*). ADRC treatment decreased infarct area in the heart in a dose-dependent manner (Fig. 1*C*). Moreover, echocardiography to assess cardiac functionality showed that ADRC treatment protected mice from cardiac dysfunction (Fig. 1*D*). The therapeutic effect afforded by ADRCs was similar to that with BM-MNCs. In addition, the treatment reduced MI-induced increases of brain natriuretic peptide (BNP) and atrial natriuretic peptide (ANP) in the heart, which are elevated in heart failure (Fig. 1, *E* and *F*), but did not recover MI-induced decreases of myosin heavy chain isoforms. Next, we investigated whether the ADRC treatment resulted in beneficial effects after MI. Notably, starting at 3–7 days after the coronary artery ligation, control mice showed increased mortality compared with the ADRC treatment group (Fig. 1*G*). Necropsy indicated that 15 of 27 mice with MI died with the presence of a blood clot within the chest cavity, which results from cardiac rupture (Fig. 1*H* and Fig. S1*A*). Conversely, ADRC treatment reduced cardiac rupture following coronary artery ligation.

The most dramatic complications of acute MI involve cardiac rupture of acutely infarcted tissue, with the tear usually preceded by a large infarct with subsequent expansion and occurring near the junction of the infarct and normal muscle (10). To examine whether ADRC treatment reduced cardiac apoptosis induced by coronary artery ligation, we identified apoptotic cardiomyocytes by terminal deoxynucleotidyl transferase dUTP nick-end labeling (TUNEL) staining of heart sections (Fig. S1*B*). ADRC treatment significantly reduced apoptosis in cardiomyocytes at 1 and 2 days following coronary artery ligation (Fig. 1*I*). Additionally, although mesenchymal stem cells secrete angiogenic factors and enhance angiogenesis in ischemic hind limbs (11), ADRC treatment did not significantly enhance angiogenesis in the heart (Fig. S1*C*). These findings suggested that ADRC treatment reduces cardiomyocyte apoptosis following coronary artery ligation, ultimately preventing MI-induced cardiac rupture.

Cardiac protection by ADRC-secreted miR-214

EVs facilitate intercellular communication in physiological and pathological processes and contain various factors, including growth factors, cytosolic signaling proteins, and extracellular matrix proteins. Exosome-meditated transfer of miRNA has emerged as a novel mechanism of genetic exchange between cells. We investigated the expression of 35 anti-apoptotic and secreted miRNAs in cardiomyocytes, BM-MNCs, and ADRCs (Table S1). Quantitative RT-PCR (qRT-PCR) revealed that these cells all express various anti-apoptotic and secreted miRNAs with miR-214 being the most abundant in ADRCs (Fig. 2*A*). qRT-PCR analysis of various tissues and cells indicated that miRNA-214 is exclusively expressed in ADRCs (Fig. 2*B*). miRNA-214 and miRNA-134 expression was significantly increased in cardiomyocytes treated with ADRC culture supernatant compared with that in controls (Fig. 2*C*); this was further increased under hypoxia conditions. *In vivo*, ADRC treatment increased miR-214 expression in the heart 1 and 2 days after coronary artery ligation (Fig. 2*D*). To examine whether miR-214 derived from ADRCs was increased in cardiomyocytes, an miR-214 inhibitor or miRNA inhibitor negative control was nucleofected into ADRCs (Fig. 2*E*). miR-214 inhibitor significantly decreased miR-214 expression in ADRCs and suppressed the increase of miR-214 expression in cardiomyocytes induced by treatment with ADRC supernatant (Fig. 2*F*), suggesting that miR-214 in the supernatant of ADRC cultures was captured in cardiomyocytes. miR-214 silencing in ADRCs significantly impaired its anti-apoptotic effects *in vitro* (Fig. 2*G*). To examine the effect of miR-214 in cardiomyocytes, rat neonatal cardiomyocytes under hypoxia were treated with an miR-214 mimic (Fig. 2*H*). This treatment significantly reduced hypoxia-induced apoptosis, suggesting that miR-214 has a protective function in cardiomyocytes. Moreover, ADRCs treated with an miR-214 inhibitor decreased the cardiac protective effects of ADRCs, whereas ADRCs treated with an miR-214 mimic enhanced the effects (Fig. 2, *I–K*). miR-214 has been shown to improve cardiomyocyte survival in MI through regulating miRNA expression, such as *Bcl2l11* and *Slc8a1* (12), potentially because miRNA association with its mRNA target generally results in target mRNA degradation (13). qRT-PCR analysis showed that the expression of *Bcl2l11* and *Slc8a1* increased 2 days after MI, whereas ADRC treatment significantly suppressed expression of these genes (Fig. 2*L*). Conversely, miR-214 blockade in ADRCs significantly impaired the ADRC-mediated effects on gene expression. These findings suggested that miR-214 secreted from ADRCs promotes cardiomyocyte survival after MI.

Clathrin-mediated endocytosis in cardiomyocytes

miRNAs secreted from cells can affect gene expression in target cells via exosomes (14). To examine whether exosomes secreted from ADRCs are transported into cardiomyocytes, exosomes were isolated from the ADRC cultures (Fig. 3*A*) and labeled with the fluorescent dye PKH67. Cardiomyocytes were then cultured with the labeled exosomes (Fig. 3*B*). Three-dimensional reconstruction of confocal microscopy images showed the labeled exosomes in the cytoplasm of the

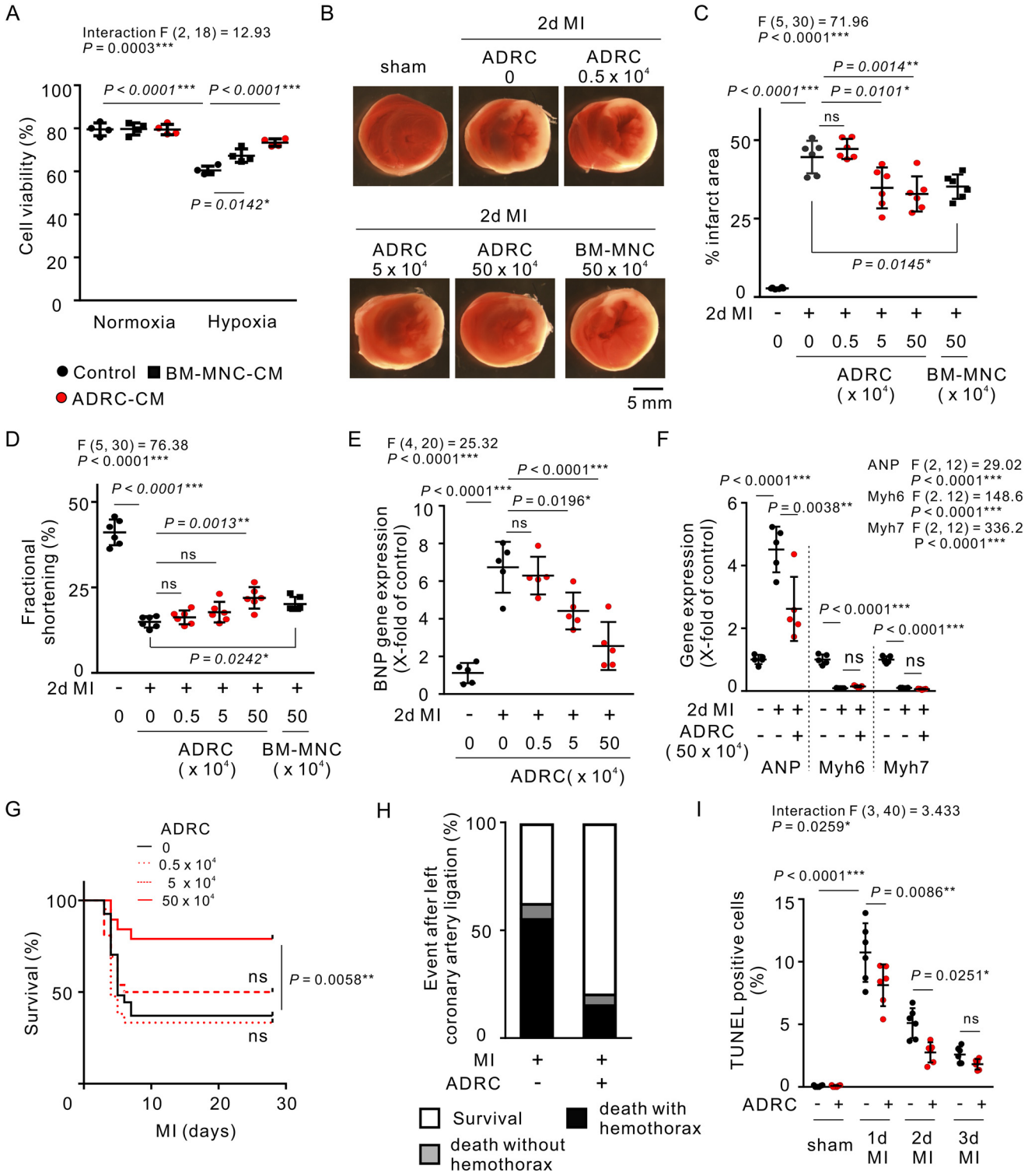

Figure 1. ADRCs protect against ischemia-induced cardiac dysfunction. *A*, cardiomyocyte cell viability in response to hypoxia as assessed by a trypan blue dye exclusion test ($n = 4$). *B*, infarct area in left ventricles 2 days after coronary artery ligation, as assessed by triphenyltetrazolium chloride staining. *C*, statistical evaluation of *B* ($n = 6$). *D*, echocardiogram analysis of left ventricular fractional shortening was performed 2 days after coronary artery ligation. *E* and *F*, gene expression in the heart 2 days after coronary artery ligation ($n = 5$). *Myh*, myosin heavy chain. *G*, survival plot up to 28 days after coronary artery ligation and ADRC injection ($n = 20–27$). *H*, percentage of survival and death with or without hemothorax after coronary artery ligation and ADRC injection ($n = 20–27$). *I*, cardiomyocyte apoptosis as assessed by a TUNEL assay in the left ventricle after coronary artery ligation and ADRC injection ($n = 6$). F and *p* values for one-way ANOVA (*C–F*) or two-way ANOVA (*A* and *I*) are shown *above* the individual *panels*. *p* values are shown for pairwise comparisons using Tukey's multiple-comparison test after ANOVA (*A*, *C–F*, and *I*). Survival curves were analyzed using Kaplan–Meyer estimators and log-rank (Mantel–Cox) testing (*G*). *ns*, not significant; *, $p < 0.05$; **, $p < 0.01$; ***, $p < 0.001$. Data are presented as the means ± standard deviation (S.D.) in all experiments.

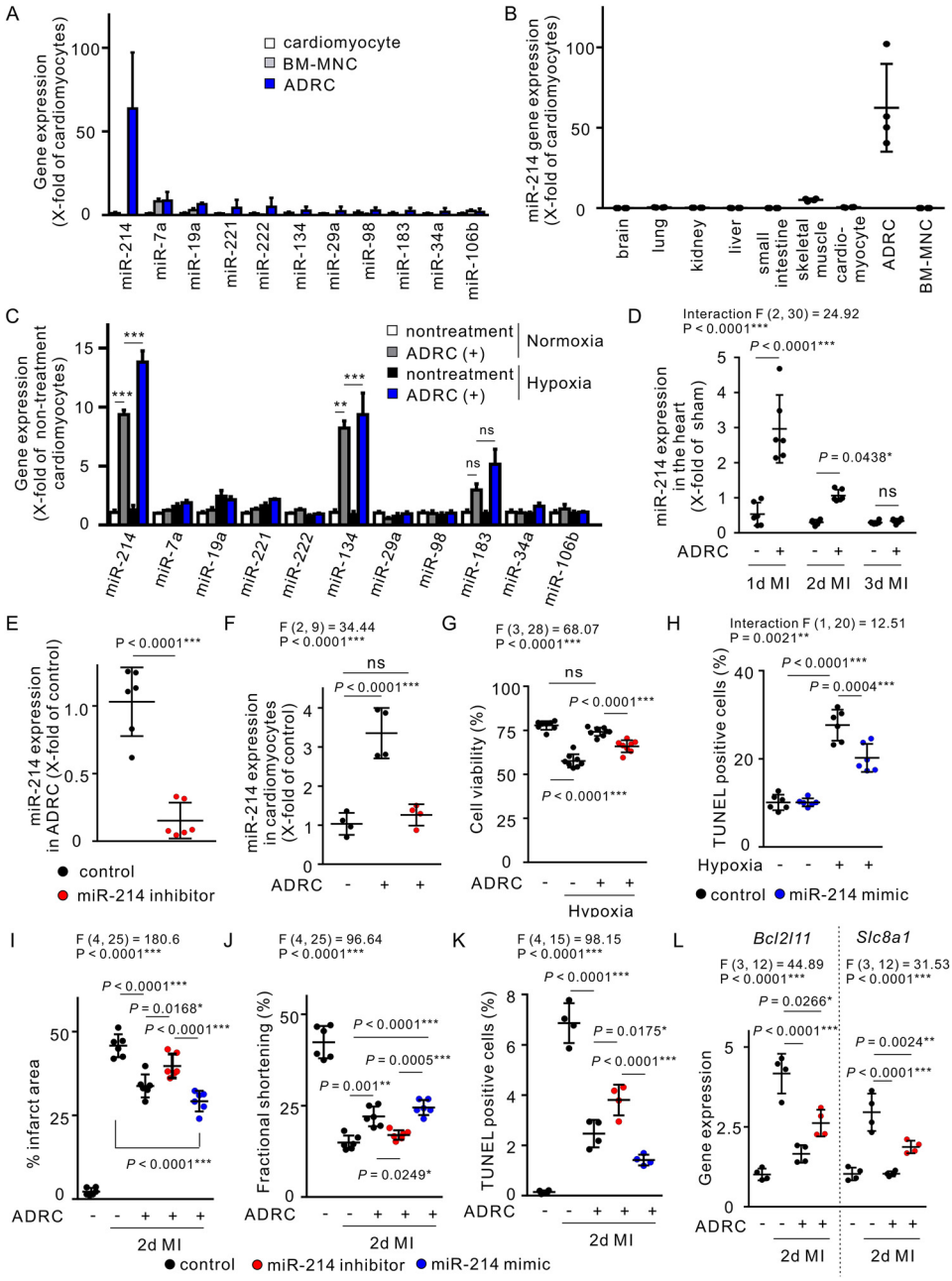

Figure 2. ADRC-secreted miR-214 reduces ischemia-induced cardiac apoptosis. *A*, anti-apoptotic and secreted miRNA expression analysis in isolated cardiomyocytes, BM-MNCs, and ADRCs using qRT-PCR ($n = 4$). *B*, tissue and cell distribution of miR-214 ($n = 4$). *C*, expression analysis of miRNAs in isolated cardiomyocytes treated with the ADRC culture supernatants ($n = 4$). Comparisons were performed using one-way ANOVA with Tukey's post hoc testing. *D*, expression analysis of miR-214 in the heart following coronary artery ligation and ADRC injection ($n = 4$). *E*, efficiency of 48-h miR-214 inhibitor–mediated miR-214 knockdown in ADRCs determined by qRT-PCR ($n = 6$). *F*, miR-214 expression in cardiomyocytes induced by ADRC culture supernatant treatment ($n = 4$). *G*, effect of miR-214 silencing in ADRCs on anti-apoptotic effects in isolated cardiomyocytes ($n = 8$). *H*, effect of an miR-214 mimic in rat neonatal cardiomyocytes ($n = 6$). *I*, infarct area in left ventricles 2 days following coronary artery ligation as assessed by triphenyltetrazolium chloride staining ($n = 6$). *J*, echocardiogram analysis of left ventricular fractional shortening. *K*, cardiomyocyte apoptosis as assessed by TUNEL assay in the left ventricle ($n = 4$). *L*, gene expression in the heart 2 days after coronary artery ligation ($n = 4$). F and *p* values for one-way ANOVA (*F*, *G*, and *I–L*) or two-way ANOVA (*D* and *H*) are shown *above* the individual *panels*. *p* values are shown for pairwise comparisons using Tukey's multiple-comparison test after ANOVA (*D* and *F–L*) or unpaired two-tailed *t* test (*E*). *ns*, not significant; *, $p < 0.05$; **, $p < 0.01$; ***, $p < 0.001$. Data are presented as the means ± standard deviation (S.D.) in all experiments.

cardiomyocytes. Hypoxia conditions increased the intensity of intracellular labeled exosomes, suggesting that hypoxia enhanced endocytosis in cardiomyocytes (Fig. 3, *C* and *D*). To examine which of the four morphologically characterized endocytic pathways (clathrin-mediated endocytosis, caveolae-mediated endocytosis, micropinocytosis, and phagocytosis) (15) mediate cell viability in cardiomyocytes under hypoxia, we investigated the effects of the inhibitors of clathrin-mediated endocytosis (chlorpromazine), caveolae-mediated endocytosis (genistein), micropinocytosis (amiloride and cytochalasin D), and phagocytosis (cytochalasin D) (Fig. 3*E*). Treatment with chlorpromazine, but not genistein, cytochalasin D, or amiloride, significantly suppressed ADRC supernatant–induced decreases of hypoxia-damaged car-

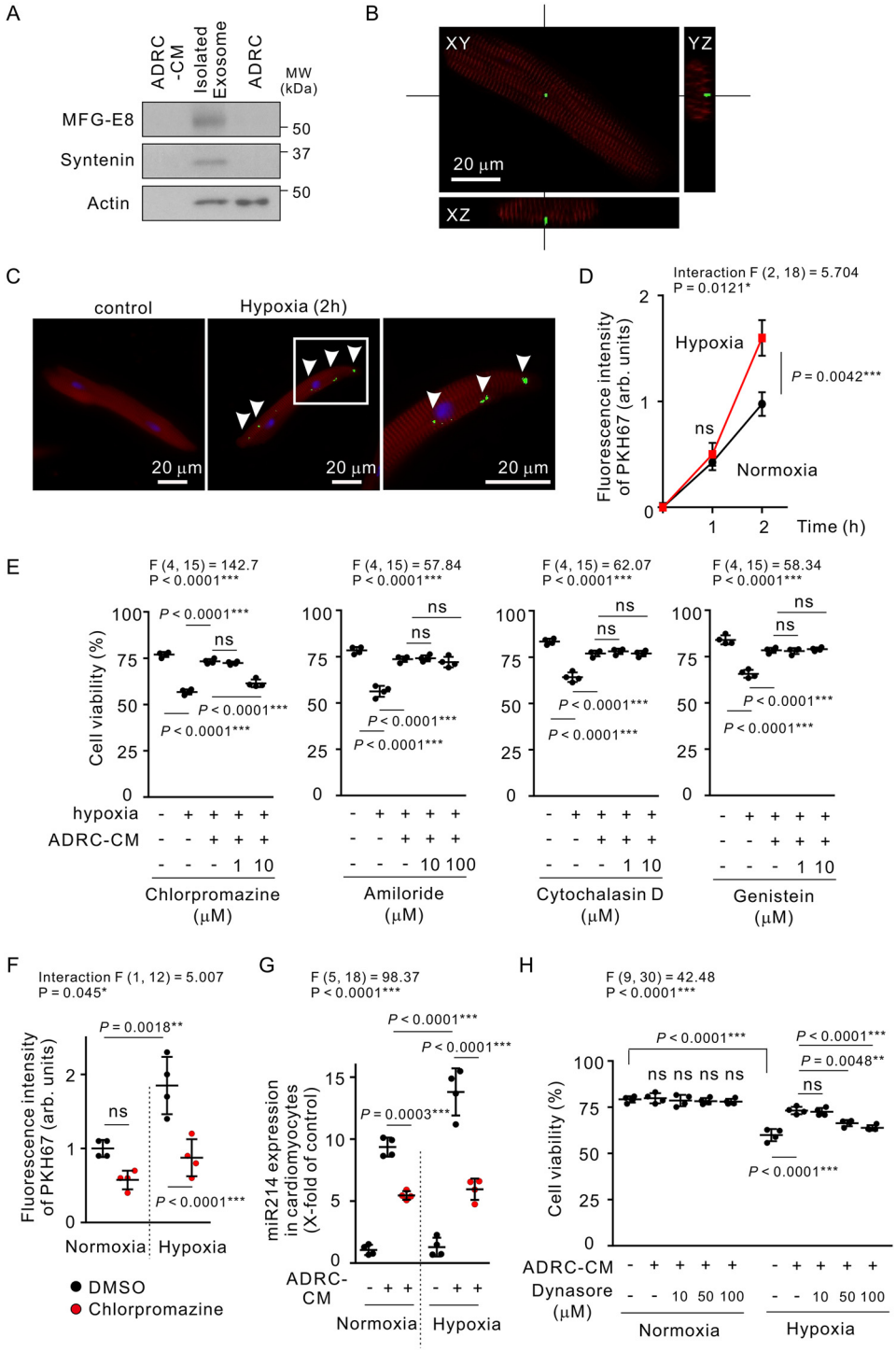

Figure 3. Hypoxia conditions activate clathrin-mediated endocytosis in cardiomyocytes. *A*, immunoblotting showing protein expression of MFG-E8, syntenin, and actin in ADRC-conditioned medium (supernatant) (*ADRC-CM*), exosomes isolated from ADRC-CM, and ADRCs. MFG-E8 and syntenin are associated with exosomes. *MW*, molecular weight. *B*, three-dimensional reconstruction of confocal microscopy images showing fluorescent dye PKH67-labeled exosomes in the cardiomyocyte cytoplasm (*red*, α-actinin; *blue*, DAPI; *green*, PKH67). *C*, hypoxia conditions enhance endocytosis in cardiomyocytes. *Right*, magnified image of the *boxed area* in the *center panel*. *D*, statistical evaluation of *C* ($n = 4$). *E*, endocytosis inhibitor–treated cardiomyocyte cell viability as assessed by the trypan blue dye exclusion test ($n = 4$). *F*, effect of chlorpromazine treatment on hypoxia-induced cardiomyocyte endocytosis ($n = 4$). *G*, qRT-PCR analysis of miR-214 expression in isolated cardiomyocytes ($n = 4$) upon chlorpromazine treatment in hypoxia conditions. *H*, effect of dynasore treatment on ADRC-CM–induced decrease of hypoxia-damaged cardiomyocytes. F and *p* values for one-way ANOVA (*E*, *G*, and *H*) or two-way ANOVA (*D* and *F*) are shown *above* the individual *panels*. *p* values are shown for pairwise comparisons using Tukey's multiple-comparison test after ANOVA (*D*–*H*). *ns*, not significant; **, $p < 0.01$; ***, $p < 0.001$.

diomyocytes. Chlorpromazine treatment decreased hypoxia-induced cardiomyocyte capture of labeled vesicles and miR-214 secreted from ADRCs (Fig. 3, *F* and *G*). Clathrin-mediated endocytosis is regulated by multiple factors, such as adaptor protein-2 (AP2) and dynamin (16). Treatment with dynasore, a cell-permeable inhibitor of dynamin, sup-

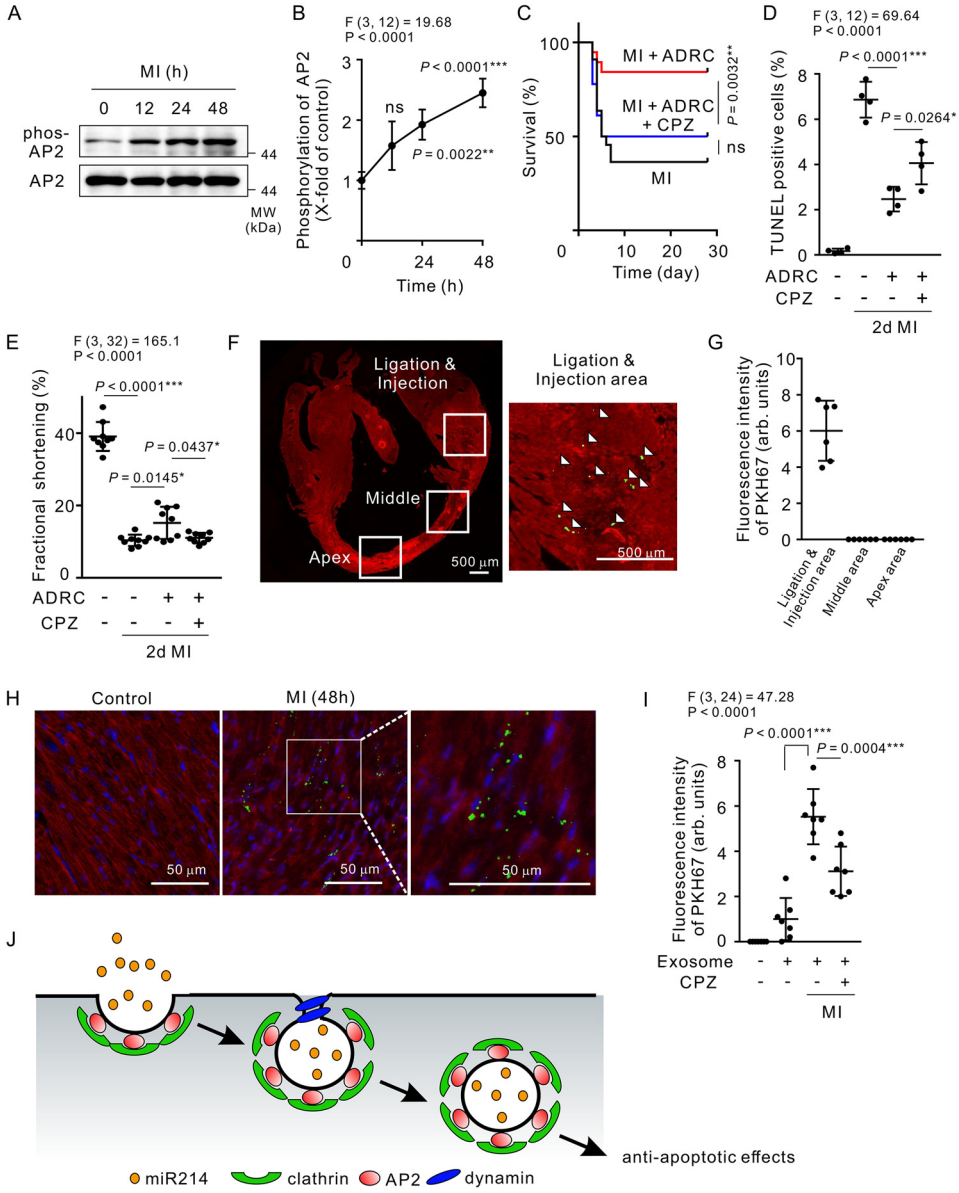

Figure 4. Clathrin-mediated endocytosis in cardiomyocytes following MI. *A*, immunoblotting showing AP2 phosphorylation in the heart following MI. *MW*, molecular weight. *B*, statistical evaluation of *A* ($n = 4$). *C*, survival plot up to 28 days following coronary artery ligation ($n = 18–27$). Effect of chlorpromazine (*CPZ*) treatment on ADRC-induced cardiac protection. *D*, results of TUNEL staining of heart sections showing the effect of CPZ on ADRC-mediated anti-apoptotic effects against MI ($n = 4$). *E*, echocardiogram analysis of left ventricular fractional shortening showing effects of chlorpromazine on ADRC-induced improvement of cardiac function ($n = 9$). *F*, cardiomyocyte endocytosis 2 days following coronary artery ligation (*red*, α-actinin; *green*, PKH67). *Right*, magnification of ligation and injection area. *G*, statistical evaluation of *F* ($n = 6$). *H*, effect of CPZ treatment on MI-induced endocytosis (*red*, α-actinin; *blue*, DAPI; *green*, PKH67). *Right*, magnification of the *boxed section* in the *central panel*. *I*, effect of CPZ treatment on cardiac endocytosis ($n = 7$). *J*, *schematic diagram* showing clathrin-mediated endocytosis. F and *p* values for one-way ANOVA (*B*, *D*, *E*, and *I*) are shown *above* the individual *panels*. *p* values are shown for pairwise comparisons from Tukey's multiple comparisons test after ANOVA (*B*, *D*, *E*, and *I*). Survival curves were analyzed using Kaplan–Meyer estimators and Log-rank (Mantel–Cox) testing (*C*). *ns*, not significant; *, $p < 0.05$; **, $p < 0.01$; ***, $p < 0.001$. Data are presented as the means ± standard deviation (S.D.) in all experiments.

pressed ADRC supernatant–induced decrease of hypoxia-damaged cardiomyocytes in a dose-dependent manner (Fig. 3*H*). These results demonstrated that clathrin-mediated endocytosis in cardiomyocytes mediates capture of vesicles including miR-214, ultimately rescuing cardiomyocytes from hypoxia damage.

Clathrin-mediated endocytosis after MI

AP2, which triggers clathrin assembly, constitutes the central node for regulating the initiation of clathrin-coated pits. Adaptor association kinase 1 (AAK1) phosphorylates AP2 at Thr-156 to stabilize the conformational changes that activate AP2. Immunoblotting showed that Thr-156 phosphorylation of AP2 in the heart increased upon MI, suggesting that clathrin-mediated endocytosis is activated under these conditions (Fig. 4, *A* and *B*). To investigate whether communication between cardiomyocytes and ADRCs affords cardiac protection through clathrin-mediated endocytosis *in vivo*, male mice were treated with ADRCs alone or in combination with chlorpromazine following coronary artery ligation (Fig. 4*C*). Notably, chlorprom-

azine treatment failed to show ADRC-induced cardiac protection (Fig. 4, *C–E*). To determine whether exosomes are transported into the cardiomyocytes *in vivo*, PKH67-labeled exosomes were injected in the heart concomitant with coronary artery ligation (Fig. 4, *F–I*). A single injection promoted the spread of PKH-labeled exosomes across an ~700 × 700 × 700-μm cubic area in the heart (Fig. 4, *F* and *G*). Among 786 PKH67-labeled exosomes in the heart, 67.7% of the PKH67-labeled exosomes were in α-actinin–positive cardiomyocytes, and 32.3% were in α-actinin–negative noncardiomyocytes or extracellular area. MI increased the intensity of the labeled exosomes in the heart, suggesting that ischemic conditions enhanced endocytosis *in vivo*. Conversely, chlorpromazine treatment suppressed the ischemia injury–induced cardiac endocytosis (Fig. 4, *H* and *I*). These results demonstrated that clathrin-mediated endocytosis is activated during acute MI and plays a critical role in communication between cardiomyocytes and ADRCs in cell-based therapy.

Discussion

miRNAs comprise a class of small regulatory RNAs that anneal with complementary sequences in target mRNAs, usually suppressing protein translation (17). Numerous studies have shown that miRNAs correlate with cardiovascular diseases (18, 19), thus constituting potential therapeutic targets (13, 20). Exosome-mediated miRNA transfer represents a novel mechanism of genetic exchange between a donor and recipient cell (21). Our qRT-PCR analysis showed that miR-214 is abundantly expressed in ADRCs and that treatment with ADRC supernatant increased its expression in cardiomyocytes and reduced cardiac rupture after acute MI. Similarly, transfection of miR-214 protects against hydrogen peroxide–induced cardiomyocyte apoptosis *in vitro* (22). Chronic miR-214 overexpression has no morphological effect on the heart (23), whereas its genetic deletion in mice increases apoptosis induced by ischemia-reperfusion and causes deterioration of cardiac function *in vivo* (24). *In vitro*, miR-214 secreted from bone marrow–derived mesenchymal stem cells protects cardiac stem cells from oxidative damage (25). We found that miR-214 secreted from ADRCs suppressed genes potentially involved in cardiac apoptosis, such as *Bcl2l11* and *Slc8a1*. For example, in response to ischemia, Bcl-2–associated X protein (Bax) activity eventually results in mitochondria-dependent cardiac myocyte death via the caspase protease system (26). The *Bcl2l11*-encoded protein induces apoptosis by activating Bax or neutralizing anti-apoptotic proteins (27). Finally, the Na^+/Ca^{2+} exchanger encoded by *Slc8A1* causes Ca^{2+} overload–associated apoptosis in cardiomyocytes under cardiac stress (24). Left ventricular rupture occurs as a consequence of excessive inflammation and matrix metalloproteinase activity after acute MI (28, 29). Although the relationship between left ventricular rupture and infarct size is unclear (30), apoptosis has been reported to be involved in left ventricular rupture after MI (31, 32). These findings suggest that miR-214–mediated anti-apoptotic effects contribute to preventing cardiac rupture.

EVs, which contain a subset of proteins, lipids, and small RNAs to facilitate cell-to-cell communication in the regulation of cancer and the immune system (14, 33), are emerging as potential therapeutic delivery agents and recognized as playing important roles in cardiac repair following MI (34). EV-mediated function in MI, the types of donor cells that secrete EVs, and their biochemical composition have been investigated (4, 8, 12). However, the particular endocytosis mechanism utilized by cardiomyocytes to obtain EV contents was unknown (35). Our findings using endocytosis inhibitors revealed that cardiomyocytes receive circulating miR-214 in EVs through clathrin-mediated endocytosis, which is regulated by multiple factors across initiation, cargo selection, maturation, and fission steps (Fig. 4*J*) (16). AP2 triggers clathrin assembly and plays a central role in endocytosis initiation (36). Specifically, AAK1-mediated AP2 phosphorylation causes conformational changes in AP2 that enhance its membrane-binding ability (37). The generation of reactive oxygen species in response to hypoxia causes phosphorylation of AP2 by AAK1 in opossum kidney cells (38). We found that AP2 was phosphorylated in the heart after MI, suggesting that hypoxia conditions may trigger clathrin-mediated endocytosis. Our data further show that dynamin, which regulates endocytic vesicle fission in the final step of clathrin-mediated endocytosis (39), contributes to the ADRC supernatant–induced decrease of hypoxia-damaged cardiomyocytes. The damaged cardiomyocytes with activated clathrin-mediated endocytosis may uptake EVs more aggressively than normal cardiomyocytes, suggesting that ADRC-derived EVs would serve as a useful tool to preferentially deliver miRNAs into the damaged cardiomyocytes. In conclusion, our data show that miRNA-214 in EVs secreted from ADRCs prevents cardiac rupture induced by acute MI and that clathrin-mediated endocytosis in cardiomyocytes plays a critical role in transporting the circulating miRNAs into the cell.

Experimental procedures

Materials and chemicals

Antibodies were used against the following proteins as follows: MFG-E8 (AF2805) from R&D Systems (Minneapolis, MN), syntenin (ab19903) and AP2M1 (ab75995) from Abcam (Cambridge, UK), phospho-AP2M1 (Thr-156; 3843S) from Cell Signaling (Beverly, MA), actin (sc-47778) from Santa Cruz Biotechnology, Inc. (Dallas, TX), and CD31 (550274) from BD Pharmingen (San Diego, CA). Inhibitors were as follows: cytochalasin D (037-17561) from Wako Pure Chemical Industries (Osaka, Japan), amiloride hydrochloride hydrate (A7410) from Sigma-Aldrich, chlorpromazine hydrochloride (08650-34) from Nacalai Tesque (Kyoto, Japan), genistein (G6649) from Sigma-Aldrich, and dynasore (sc-202592) from Santa Cruz Biotechnology. TUNEL staining was performed using the In Situ Cell Death detection kit (Roche Diagnostics).

In vitro experiments

Adult mouse cardiomyocytes were isolated as described previously (40). The culture media were removed, and adherent cells were cultured with DMEM or conditioned medium from ADRCs or BM-MNCs. Inhibitors were added at 1 h after cell plating and mixed with DMEM or conditioned medium. For hypoxia studies, cells were exposed to hypoxia for 6 h. Hypoxic conditions were generated by using an AnaeroPack system

(Mitsubishi GAS Chemical, Tokyo, Japan). Neonatal rat ventricular myocytes (NRVMs) were isolated from 1–2-day-old rat neonates (41). Primary NRVMs were incubated in DMEM with 10% fetal bovine serum.

Cell viability was assessed by a trypan blue exclusion assay. In 6 h of culture under normoxic or hypoxic conditions, trypan blue (0.4%; Gibco) was added into the culture dish (final concentration, 0.04%). The number of viable (unstained) and nonviable (blue-stained) cells was recorded in 10 random microscopic fields.

To study the pathway of exosome uptake *in vitro*, cells were preincubated with an inhibitor for 30 min prior to adding conditioned medium with exosomes and then incubated with an inhibitor. Cytochalasin D (1–10 μmol/liter), 10–100 μmol/liter amiloride, 1–10 μmol/liter chlorpromazine, 1–10 μmol/liter genistein, or 10–100 μmol/liter dynasore was used. Cytochalasin D, amiloride, genistein, and dynasore were dissolved in DMSO (final concentration $< 0.1\%$).

Animal experiments

MI was induced in 8-week-old male C57BL/6J mice (Nihon Crea, Tokyo, Japan) as described previously (42). After the left anterior descending artery was ligated, mice were administered an intramyocardial injection of cells (60 μl of 0.5×10^4, 5×10^4, or 50×10^4 ADRCs in PBS) or PBS alone (60 μl) into two infarct border zones and two infarct zones (15 μl in each site) with a 30-gauge needle. Mice were sacrificed at 2 or 28 days after surgery. The heart was incubated with TTC to determine the infarcted area. Transthoracic echocardiography was performed on mice using a Vevo 1100 (Fujifilm VisualSonica Inc., Bothell, WA) with a 40-MHz probe. The cause of death was determined by necropsy, and cardiac rupture was diagnosed by the presence of a blood clot within the chest cavity as described previously (43).

mRNA and microRNA expression analysis

To analyze mRNA expression, RNA was extracted from peri-infarcted areas in the left ventricle using an RNeasy Mini kit (Qiagen, Chatsworth, CA) following the manufacturer's protocol and reverse-transcribed using the ReverTra Ace qPCR RT Master Mix (Toyobo, Osaka, Japan). qRT-PCR analysis was assessed using SYBR Premix Ex TaqII (TaKaRa Bio, Shiga, Japan) and the following primers: *Nppb* (BNP), 5′-AGC TGC TTT GGG CAC AAG ATA GA-3′ and 5′-ATC ACT TCA AAG GTG GTC CCA GA-3′; *Nppa* (ANP), 5′-TGA CAG GAT TGG AGC CCA GA-3′ and 5′-GAC ACA CCA CAA GGG CTT AGG A-3′; *Myh6*, 5′-CGC AAT GCA GAG TCG GTG A-3′ and 5′-TCC TGC AGC CGC ATTA AGT TC-3′; *Myh7*, 5′-ATG CAG GAC CTG GTG GAC A-3′ and 5′-CTT GCG GTA CTT AGC CAG GTT G-3′; *Slc8a1*, 5′-TTG GCT GCA CCA TTG GTC TGA AAG-3′ and 5′- ACA CTT TGA ACT GTT CCC CGT TGG-3′; *Bcl2l11*, 5′-GGA GAC GAG TTC AAC GAA ACT T-3′ and 5′-AAC AGT TGT AAG ATA ACC ATT TGA GG-3′; *Gapdh*, 5′-TGT GTC CGT GGA TCT GA-3′ and 5′-TTG CTG TTG AAG TCG CAG GAG-3′. Data are presented following normalization with *Gapdh*.

MicroRNA was obtained by using the miRNeasy Micro kit (Qiagen) and reverse-transcribed to cDNA using the miScript II RT Kit (Qiagen) following the manufacturer's protocol. qRT-PCR analysis was performed using the miScript SYBR Green PCR kit (Qiagen) with the miScript universal primer and miRNA-specific forward primers. All miScript Primer Assays (see Table S1) were purchased from Qiagen. Data are presented following normalization with *Rnu6b*.

MicroRNA inhibitor and mimic

ADRCs were transfected with 10 nmol/liter mirVana miR-214 inhibitor (si-miR214) or 10 nmol/liter miR-214 mimic (mmu-miR-214) (Thermo Fisher Scientific) using a Lipofectamine RNAiMAX system (Thermo Fisher Scientific) by following the manufacturer's protocol. MirVana miRNA inhibitor negative control 1 (si-miR-scramble) was used as a negative control. NRVMs were transfected with 10 nmol/liter mirVana miR-214 mimic (rno-miR-214) (Thermo Fisher Scientific) using a Lipofectamine RNAiMAX system by following the manufacturer's protocol.

Isolation and analysis of exosomes

ADRCs were cultured in DMEM supplemented with 10% exosome-depleted fetal bovine serum (Gibco, A25904DG) over 48 h. ADRC-derived exosomes were isolated from the conditioned medium of ADRCs using ExoQuick-TC exosome precipitation solution (EXOTC10A-1, System Biosciences, Palo Alto, CA) following the manufacturer's protocol. The protein levels of MFG-E8 and syntenin, a representative marker of exosomes, were detected by Western blotting.

Exosome labeling and uptake by cardiomyocytes

ADRC-derived exosomes were labeled using the PKH-67 green fluorescent cell linker kit (PKH67GL, Sigma-Aldrich). Following incubation for 5 min, exosomes were washed several times using an Amicon Ultra-0.5 centrifugal filter device (nominal molecular weight limit 100,000) (Millipore, Billerica, MA). Adult mouse cardiomyocytes were incubated with the labeled exosomes for 1–2 h with or without hypoxia. Exosome uptake was quantified as a percentage of fluorescence intensity relative to the reference of 2-h culture without hypoxia. Exosome localization was viewed using a BZ-X710 microscope (Keyence, Osaka, Japan) with a sectioning technique.

To study exosome uptake *in vivo*, mice were administered an intramyocardial injection of ADRC-derived exosomes into two infarct border zones (15 μl in each site) following MI. Some mice were injected with the mixture of exosomes and 10 μmol/liter chlorpromazine to study the pathway of exosome uptake. Cellular uptake of ADRC-derived exosomes by cardiomyocytes was observed using a BZ-X710 microscope. Exosome uptake was quantified as the percentage of fluorescence intensity relative to the reference of sham mice injected with exosomes without 10 μmol/liter chlorpromazine.

Study approval

All procedures of animal care and animal use in this study were approved by the Animal Ethics Review Board of Nagoya University School of Medicine.

Statistical analysis

Data are presented as the means ± S.D. for given experiments. All statistical analyses for experiments were performed using GraphPad Prism 6 (GraphPad Software, La Jolla, CA). Comparisons between two groups were performed using an unpaired Student's *t* test, whereas those between more than two groups utilized ANOVA with Tukey's post hoc testing. Survival curves were analyzed with Kaplan–Meyer estimators and log-rank (Mantel–Cox) testing. Significance was defined as $p < 0.05$ (*, $p < 0.05$; **, $p < 0.01$; ***, $p < 0.001$).

Author contributions—S. E. and M. T. designed the experiments. S. E., T. S., S. I., Y. M., T. Tsuda, T. Takikawa, and T. Y. performed the animal and *in vitro* experiments. R. H., Y. S., and K. K. contributed to isolation of ADRCs. S. E. and M. T. wrote the manuscript, with contributions from K. O., Y. B., N. O., and T. M.

Acknowledgments—We thank the staff from the Division of Experimental Animals, Nagoya University School of Medicine, for assisting with animal experiments.

References

1. Yeh, R. W., Sidney, S., Chandra, M., Sorel, M., Selby, J. V., and Go, A. S. (2010) Population trends in the incidence and outcomes of acute myocardial infarction. *N. Engl. J. Med.* **362,** 2155–2165 CrossRef Medline
2. Gyöngyösi, M., Haller, P. M., Blake, D. J., and Martin Rendon, E. (2018) Meta-analysis of cell therapy studies in heart failure and acute myocardial infarction. *Circ. Res.* **123,** 301–308 CrossRef Medline
3. Gyöngyösi, M., Wojakowski, W., Navarese, E. P., Moye, L. À., and ACCRUE Investigators (2016) Meta-analyses of human cell-based cardiac regeneration therapies: controversies in meta-analyses results on cardiac cell-based regenerative studies. *Circ. Res.* **118,** 1254–1263 CrossRef Medline
4. Barile, L., Moccetti, T., Marbán, E., and Vassalli, G. (2017) Roles of exosomes in cardioprotection. *Eur. Heart J.* **38,** 1372–1379 CrossRef Medline
5. Smith, R. R., Barile, L., Cho, H. C., Leppo, M. K., Hare, J. M., Messina, E., Giacomello, A., Abraham, M. R., and Marbán, E. (2007) Regenerative potential of cardiosphere-derived cells expanded from percutaneous endomyocardial biopsy specimens. *Circulation* **115,** 896–908 CrossRef Medline
6. Chimenti, I., Smith, R. R., Li, T. S., Gerstenblith, G., Messina, E., Giacomello, A., and Marbán, E. (2010) Relative roles of direct regeneration versus paracrine effects of human cardiosphere-derived cells transplanted into infarcted mice. *Circ. Res.* **106,** 971–980 CrossRef Medline
7. Gnecchi, M., Zhang, Z., Ni, A., and Dzau, V. J. (2008) Paracrine mechanisms in adult stem cell signaling and therapy. *Circ. Res.* **103,** 1204–1219 CrossRef Medline
8. Suzuki, E., Fujita, D., Takahashi, M., Oba, S., and Nishimatsu, H. (2016) Stem cell-derived exosomes as a therapeutic tool for cardiovascular disease. *World J. Stem Cells* **8,** 297–305 CrossRef Medline
9. Gray, W. D., French, K. M., Ghosh-Choudhary, S., Maxwell, J. T., Brown, M. E., Platt, M. O., Searles, C. D., and Davis, M. E. (2015) Identification of therapeutic covariant microRNA clusters in hypoxia-treated cardiac progenitor cell exosomes using systems biology. *Circ. Res.* **116,** 255–263 CrossRef Medline
10. Zipes, D. P., Libby, P., Bonow, R. O., Mann, D. L., and Tomaselli, G. F. (2019) *Braunwald's Heart Disease: A Textbook of Cardiovascular Medicine*, 11th Ed., Elsevier, Philadelphia
11. Li, Y., Liu, W., Liu, F., Zeng, Y., Zuo, S., Feng, S., Qi, C., Wang, B., Yan, X., Khademhosseini, A., Bai, J., and Du, Y. (2014) Primed 3D injectable microniches enabling low-dosage cell therapy for critical limb ischemia. *Proc. Natl. Acad. Sci. U.S.A.* **111,** 13511–13516 CrossRef Medline
12. Boon, R. A., and Dimmeler, S. (2015) MicroRNAs in myocardial infarction. *Nat. Rev. Cardiol.* **12,** 135–142 CrossRef Medline
13. van Rooij, E., and Olson, E. N. (2012) MicroRNA therapeutics for cardiovascular disease: opportunities and obstacles. *Nat. Rev. Drug Discov.* **11,** 860–872 CrossRef Medline
14. Colombo, M., Raposo, G., and Théry, C. (2014) Biogenesis, secretion, and intercellular interactions of exosomes and other extracellular vesicles. *Annu. Rev. Cell Dev. Biol.* **30,** 255–289 CrossRef Medline
15. Khalil, I. A., Kogure, K., Akita, H., and Harashima, H. (2006) Uptake pathways and subsequent intracellular trafficking in nonviral gene delivery. *Pharmacol. Rev.* **58,** 32–45 CrossRef Medline
16. Mettlen, M., Chen, P. H., Srinivasan, S., Danuser, G., and Schmid, S. L. (2018) Regulation of clathrin-mediated endocytosis. *Annu. Rev. Biochem.* **87,** 871–896 CrossRef Medline
17. Ha, M., and Kim, V. N. (2014) Regulation of microRNA biogenesis. *Nat. Rev. Mol. Cell Biol.* **15,** 509–524 CrossRef Medline
18. Akat, K. M., Moore-McGriff, D., Morozov, P., Brown, M., Gogakos, T., Correa Da Rosa, J., Mihailovic, A., Sauer, M., Ji, R., Ramarathnam, A., Totary-Jain, H., Williams, Z., Tuschl, T., and Schulze, P. C. (2014) Comparative RNA-sequencing analysis of myocardial and circulating small RNAs in human heart failure and their utility as biomarkers. *Proc. Natl. Acad. Sci. U.S.A.* **111,** 11151–11156 CrossRef Medline
19. Zampetaki, A., and Mayr, M. (2012) MicroRNAs in vascular and metabolic disease. *Circ. Res.* **110,** 508–522 CrossRef Medline
20. Wahlquist, C., Jeong, D., Rojas-Muñoz, A., Kho, C., Lee, A., Mitsuyama, S., van Mil, A., Park, W. J., Sluijter, J. P., Doevendans, P. A., Hajjar, R. J., and Mercola, M. (2014) Inhibition of miR-25 improves cardiac contractility in the failing heart. *Nature* **508,** 531–535 CrossRef Medline
21. Valadi, H., Ekström, K., Bossios, A., Sjöstrand, M., Lee, J. J., and Lötvall, J. O. (2007) Exosome-mediated transfer of mRNAs and microRNAs is a novel mechanism of genetic exchange between cells. *Nat. Cell Biol.* **9,** 654–659 CrossRef Medline
22. Lv, G., Shao, S., Dong, H., Bian, X., Yang, X., and Dong, S. (2014) MicroRNA-214 protects cardiac myocytes against H_2O_2-induced injury. *J. Cell. Biochem.* **115,** 93–101 CrossRef Medline
23. van Rooij, E., Sutherland, L. B., Liu, N., Williams, A. H., McAnally, J., Gerard, R. D., Richardson, J. A., and Olson, E. N. (2006) A signature pattern of stress-responsive microRNAs that can evoke cardiac hypertrophy and heart failure. *Proc. Natl. Acad. Sci. U.S.A.* **103,** 18255–18260 CrossRef Medline
24. Aurora, A. B., Mahmoud, A. I., Luo, X., Johnson, B. A., van Rooij, E., Matsuzaki, S., Humphries, K. M., Hill, J. A., Bassel-Duby, R., Sadek, H. A., and Olson, E. N. (2012) MicroRNA-214 protects the mouse heart from ischemic injury by controlling Ca^{2+} overload and cell death. *J. Clin. Invest.* **122,** 1222–1232 CrossRef Medline
25. Wang, Y., Zhao, R., Liu, D., Deng, W., Xu, G., Liu, W., Rong, J., Long, X., Ge, J., and Shi, B. (2018) Exosomes derived from miR-214-enriched bone marrow-derived mesenchymal stem cells regulate oxidative damage in cardiac stem cells by targeting CaMKII. *Oxid. Med. Cell Longev.* **2018,** 4971261 CrossRef Medline
26. Baines, C. P. (2010) The cardiac mitochondrion: nexus of stress. *Annu. Rev. Physiol.* **72,** 61–80 CrossRef Medline
27. Shukla, S., Saxena, S., Singh, B. K., and Kakkar, P. (2017) BH3-only protein BIM: an emerging target in chemotherapy. *Eur. J. Cell Biol.* **96,** 728–738 CrossRef Medline
28. Fang, L., Gao, X. M., Moore, X. L., Kiriazis, H., Su, Y., Ming, Z., Lim, Y. L., Dart, A. M., and Du, X. J. (2007) Differences in inflammation, MMP activation and collagen damage account for gender difference in murine cardiac rupture following myocardial infarction. *J. Mol. Cell Cardiol.* **43,** 535–544 CrossRef Medline
29. Anzai, T. (2013) Post-infarction inflammation and left ventricular remodeling: a double-edged sword. *Circ. J.* **77,** 580–587 CrossRef Medline
30. Gao, X. M., Ming, Z., Su, Y., Fang, L., Kiriazis, H., Xu, Q., Dart, A. M., and Du, X. J. (2010) Infarct size and post-infarct inflammation determine the risk of cardiac rupture in mice. *Int. J. Cardiol.* **143,** 20–28 CrossRef Medline
31. Matsusaka, H., Ide, T., Matsushima, S., Ikeuchi, M., Kubota, T., Sunagawa, K., Kinugawa, S., and Tsutsui, H. (2006) Targeted deletion of p53 prevents cardiac rupture after myocardial infarction in mice. *Cardiovasc. Res.* **70,** 457–465 CrossRef Medline

32. Barandon, L., Couffinhal, T., Ezan, J., Dufourcq, P., Costet, P., Alzieu, P., Leroux, L., Moreau, C., Dare, D., and Duplàa, C. (2003) Reduction of infarct size and prevention of cardiac rupture in transgenic mice overexpressing FrzA. *Circulation* **108,** 2282–2289 CrossRef Medline
33. Robbins, P. D., Dorronsoro, A., and Booker, C. N. (2016) Regulation of chronic inflammatory and immune processes by extracellular vesicles. *J. Clin. Invest.* **126,** 1173–1180 CrossRef Medline
34. Sahoo, S., and Losordo, D. W. (2014) Exosomes and cardiac repair after myocardial infarction. *Circ. Res.* **114,** 333–344 CrossRef Medline
35. Conner, S. D., and Schmid, S. L. (2003) Regulated portals of entry into the cell. *Nature* **422,** 37–44 CrossRef Medline
36. Traub, L. M. (2009) Tickets to ride: selecting cargo for clathrin-regulated internalization. *Nat. Rev. Mol. Cell Biol.* **10,** 583–596 CrossRef Medline
37. Ricotta, D., Conner, S. D., Schmid, S. L., von Figura, K., and Honing, S. (2002) Phosphorylation of the AP2 μ subunit by AAK1 mediates high affinity binding to membrane protein sorting signals. *J. Cell Biol.* **156,** 791–795 CrossRef Medline
38. Chen, Z., Krmar, R. T., Dada, L., Efendiev, R., Leibiger, I. B., Pedemonte, C. H., Katz, A. I., Sznajder, J. I., and Bertorello, A. M. (2006) Phosphorylation of adaptor protein-2 mu2 is essential for Na^+,K^+-ATPase endocytosis in response to either G protein-coupled receptor or reactive oxygen species. *Am. J. Respir. Cell Mol. Biol.* **35,** 127–132 CrossRef Medline
39. Antonny, B., Burd, C., De Camilli, P., Chen, E., Daumke, O., Faelber, K., Ford, M., Frolov, V. A., Frost, A., Hinshaw, J. E., Kirchhausen, T., Kozlov, M. M., Lenz, M., Low, H. H., McMahon, H., *et al.* (2016) Membrane fission by dynamin: what we know and what we need to know. *EMBO J.* **35,** 2270–2284 CrossRef Medline
40. Wolska, B. M., and Solaro, R. J. (1996) Method for isolation of adult mouse cardiac myocytes for studies of contraction and microfluorimetry. *Am. J. Physiol.* **271,** H1250–H1255 CrossRef Medline
41. Takefuji, M., Wirth, A., Lukasova, M., Takefuji, S., Boettger, T., Braun, T., Althoff, T., Offermanns, S., and Wettschureck, N. (2012) G(13)-mediated signaling pathway is required for pressure overload-induced cardiac remodeling and heart failure. *Circulation* **126,** 1972–1982 CrossRef Medline
42. Kobayashi, K., Luo, M., Zhang, Y., Wilkes, D. C., Ge, G., Grieskamp, T., Yamada, C., Liu, T. C., Huang, G., Basson, C. T., Kispert, A., Greenspan, D. S., and Sato, T. N. (2009) Secreted Frizzled-related protein 2 is a procollagen C proteinase enhancer with a role in fibrosis associated with myocardial infarction. *Nat. Cell Biol.* **11,** 46–55 CrossRef Medline
43. Korf-Klingebiel, M., Kempf, T., Schlüter, K. D., Willenbockel, C., Brod, T., Heineke, J., Schmidt, V. J., Jantzen, F., Brandes, R. P., Sugden, P. H., Drexler, H., Molkentin, J. D., and Wollert, K. C. (2011) Conditional transgenic expression of fibroblast growth factor 9 in the adult mouse heart reduces heart failure mortality after myocardial infarction. *Circulation* **123,** 504–514 CrossRef Medline

Cardiomyocytes capture stem cell-derived, anti-apoptotic microRNA-214 via clathrin-mediated endocytosis in acute myocardial infarction

Shunsuke Eguchi, Mikito Takefuji, Teruhiro Sakaguchi, Sohta Ishihama, Yu Mori, Takuma Tsuda, Tomonobu Takikawa, Tatsuya Yoshida, Koji Ohashi, Yuuki Shimizu, Ryo Hayashida, Kazuhisa Kondo, Yasuko K. Bando, Noriyuki Ouchi and Toyoaki Murohara

J. Biol. Chem. 2019, 294:11665-11674.
doi: 10.1074/jbc.RA119.007537 originally published online June 19, 2019

Cardiomyocytes capture stem cell-derived, anti-apoptotic microRNA-214 via clathrin-mediated endocytosis in acute myocardial infarction

Shunsuke Eguchi, Mikito Takefuji*, Teruhiro Sakaguchi, Sohta Ishihama, Yu Mori, Takuma Tsuda, Tomonobu Takikawa, Tatsuya Yoshida, Koji Ohashi, Yuuki Shimizu, Ryo Hayashida, Kazuhisa Kondo, Yasuko K. Bando, Noriyuki Ouchi, Toyoaki Murohara*

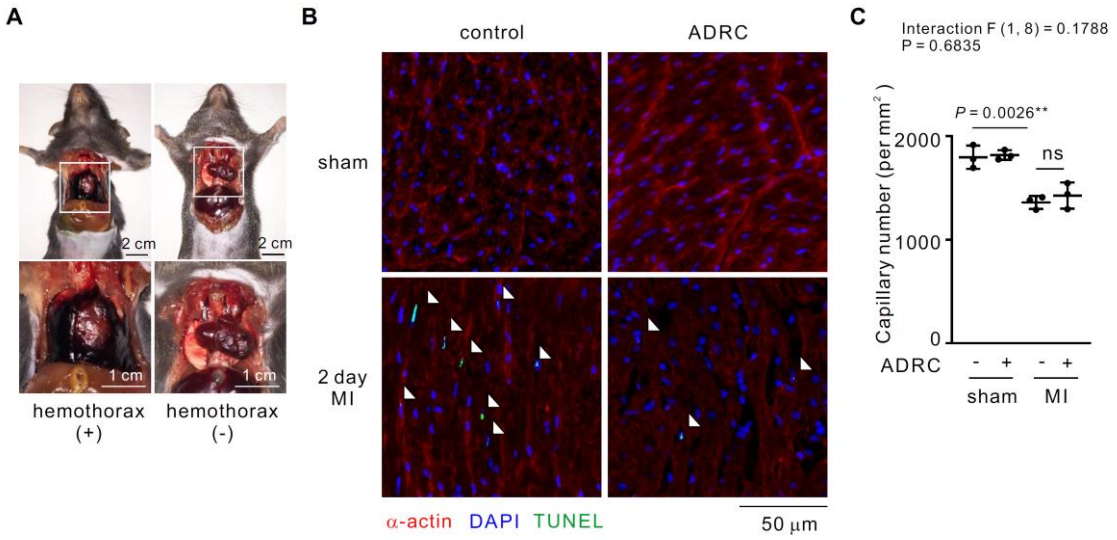

Figure S1. Adipose-Derived Regenerative Cells (ADRCs) protect against ischemia-induced cardiac dysfunction. (**A**) Myocardial infarction (MI)-associated death with the presence of a blood clot within the chest cavity, which results from cardiac rupture. (**B**) Cardiomyocyte apoptosis as assessed by TUNEL assay in the left ventricle two days after ligating the coronary artery. (**C**) Capillary densities in the heart were examined by staining the heart sections with an anti-CD31 antibody. Effect of ADRC-treatment on angiogenesis is shown. F and P values for two-way ANOVA are shown above individual panels. *P* values are shown for pairwise comparisons using Tukey's multiple comparisons test after ANOVA. ns, not significant; $^{**}P < 0.01$.

Table S1. PCR primers used for detection of miRNAs.

miRNA	Product information	Catalogue number
miR-7a	Mm_miR-7_1 miScript Primer Assay	MS00005880
miR-9	Mm_miR-9_1 miScript Primer Assay	MS00012873
miR-17	Mm_miR-17_1 miScript Primer Assay	MS00011256
miR-19a	Mm_miR-19a_1 miScript Primer Assay	MS00001302
miR-23a	Mm_miR-23a_2 miScript Primer Assay	MS00032599
miR-24	Mm_miR-24_1 miScript Primer Assay	MS00005922
miR-25	Mm_miR-25_1 miScript Primer Assay	MS00001337
miR-26b	Mm_miR-26b_1 miScript Primer Assay	MS00001344
miR-27a	Mm_miR-27a_1 miScript Primer Assay	MS00001351
miR-29a	Mm_miR-29a_1 miScript Primer Assay	MS00001372
miR-29b	Mm_miR-29b_1 miScript Primer Assay	MS00005936
miR-30a	Mm_miR-30a_1 miScript Primer Assay	MS00011704
miR-30b	Mm_miR-30b_1 miScript Primer Assay	MS00001386
miR-30c	Mm_miR-30c_2 miScript Primer Assay	MS00011725
miR-30d	Mm_miR-30d_2 miScript Primer Assay	MS00011746
miR-30e	Mm_miR-30e_2 miScript Primer Assay	MS00011753
miR-34a	Mm_miR-34a_1 miScript Primer Assay	MS00001428
miR-92a	Mm_miR-92_1 miScript Primer Assay	MS00005971
miR-98	Mm_miR-98_1 miScript Primer Assay	MS00001463
miR-101a	Mm_miR-101a_3 miScript Primer Assay	MS00011011
miR-106b	Mm_miR-106b_1 miScript Primer Assay	MS00001512
miR-134	Mm_miR-134_1 miScript Primer Assay	MS00001568
miR-150	Mm_miR-150_1 miScript Primer Assay	MS00001673
miR-181c	Mm_miR-181c_3 miScript Primer Assay	MS00032382
miR-183	Mm_miR-183_1 miScript Primer Assay	MS00001722
miR-20	Mm_miR-205_1 miScript Primer Assay	MS00001862
miR-210	Mm_miR-210_2 miScript Primer Assay	MS00032564
miR-214	Mm_miR-214_2 miScript Primer Assay	MS00032571
miR-221	Mm_miR-221_2 miScript Primer Assay	MS00032585
miR-222	Mm_miR-222_2 miScript Primer Assay	MS00007959
miR-351	Mm_miR-351_1 miScript Primer Assay	MS00002219
miR-378a	Mm_miR-378_2 miScript Primer Assay	MS00032781
miR-497a	Mm_miR-497_1 miScript Primer Assay	MS00002569
miR-503	Mm_miR-503_1 miScript Primer Assay	MS00002597
let-7e	Mm_let-7e_3 miScript Primer Assay	MS00032186
Rnu6b	Hs_RNU6-2_11 miScript Primer Assay	MS00033740